Journal of Luminescence 136 (2013) 358–364

Contents lists available at SciVerse ScienceDirect

Journal of Luminescence

journal homepage: www.elsevier.com/locate/jlumin

Annihilation of the triplet excitons in the nanoporous glass matrices

D.A. Afanasyev [a,*], N.Kh. Ibrayev [a], A.M. Saletsky [b], Y.V. Starokurov [b], V.M. Gun'ko [c], S.V. Mikhalovsky [d,e]

[a] Institute of Molecular Nanophotonics, Buketov Karaganda State University, Universitetskaya Street 28, Karaganda 100028, Kazakhstan
[b] Faculty of Physics, Lomonosov Moscow State University, 1-2 Leninskie Gory, Moscow 119991, Russian Federation
[c] Chuiko Institute of Surface Chemistry, 17 General Naumov Street, Kiev 03164, Ukraine
[d] School of Pharmacy and Biomolecular Sciences, University of Brighton, Cockcroft Building, Lewes Road, Brighton BN2 4GJ, United Kingdom
[e] School of Engineering, Nazarbayev University, 53 Kabanbay Batyr Avenue, Astana 010000, Kazakhstan

ARTICLE INFO

Article history:
Received 1 June 2012
Received in revised form
27 October 2012
Accepted 6 November 2012
Available online 29 November 2012

Keywords:
Delayed fluorescence
Triplet–triplet annihilation
Magnetic field effect
Porous glasses
Molecular clusters

ABSTRACT

The spectra and kinetics of fluorescence decay of 1,2-benzanthracene (1,2-BA) molecular clusters adsorbed in nanoporous borosilicate glasses were investigated. It has been shown that the type of the decay kinetics of delayed fluorescence is determined by the annihilation of triplet excitons in crystalline and percolation clusters. The influence of an external magnetic field on the annihilation rate constant of triplet excitons in the adsorbed 1,2-BA molecules has been studied. The response of the molecular clusters to the magnetic field strongly depends on temperature, pore size and time scale of the observation. Clusters with the crystal structure dominate in the decay kinetics of triplet–triplet annihilation (TTA) and delayed fluorescence in the initial microsecond period of time after excitation. Amorphous clusters determine the form of decay kinetics of delayed fluorescence in the millisecond range. The increase in the pore size and concentration of the adsorbate lead to the dominance of crystalline components. The results presented here can be used to develop techniques for probing the structure of the adsorbed layer in nanoporous systems examining the effect of an external magnetic field on the annihilation delayed fluorescence (ADF) kinetics.

1. Introduction

Processes of transformation of electronic excitation energy in homogeneous bulk media are well studied, both theoretically and experimentally [1,2]. Effects of the confined space on these phenomena have received less attention, although such objects include porous matrices, colloids, micelles, Langmuir–Blodgett (LB) films and nanoparticles. Common to all of them is the fact that the dimensions of the confined space, in which these processes take place, are comparable to the size of the embedded species and the photoreaction kinetics in such systems cannot be described by classic equations of formal chemical kinetics [3,4]. At present, interest to photoprocesses in confined space at nanoscale is rising owing to the progress in nanotechnology and nanomaterials. One can expect to observe non-traditional kinetics for molecular reactions in small spatial domains of nanostructured systems [5–9].

The reaction of spin-selective triplet–triplet annihilation can influence the optical properties of molecular crystals [10,11], liquid solutions [12,13], polymers [14], and micellar systems [15]. The role of TTA in deactivation of the excited electronic states of electroluminescent substances was proven [16,17].

Theoretical models of TTA in homogeneous environments were developed in the classic works [10,13,18,19]. In Refs. [20,21] the competitive effect of the magnetic field and the external heavy atom on the TTA in solution was experimentally studied. The theoretical interpretation of the effects of the spin–orbit interaction and magnetic field in the triplet pairs were given in Refs. [22–25]. In Ref. [26], the larger change in the intensity of the annihilation delayed fluorescence in the magnetic field was registered for two-component systems. It was explained by the fact that the annihilation proceeds through the stage of charge transfer [22].

More refined interpretation of experimental data on TTA was presented later [27–30]. The system dimension effects in TTA were studied [4,31,32]. Using the statistical approach and a Monte-Carlo method it was shown that the TTA rate constant depends on the dimension. The nonexponential kinetics of triplet–triplet annihilation delayed fluorescence in LB films was described using a combination of formal-kinetics and percolation models [33,34]. The effect of disorder on the process of TTA and the values of the observed magnetic effects are given in Ref. [35]. Simple analytical

* Corresponding author. Tel.: +7 7212 770446; fax: +7 7212 770384.
E-mail addresses: a_d_afanasyev@mail.ru (D.A. Afanasyev), niazibraev@mail.ru (N.Kh. Ibrayev).

0022-2313/$ - see front matter © 2012 Elsevier B.V. All rights reserved.
http://dx.doi.org/10.1016/j.jlumin.2012.11.013

expressions are given in this article. They allow to estimate the degree of disorder of the structure and total annihilation probability.

It is known that annihilation of triplet excitons proceeds according to the following reaction:

TTA process is sensitive to the external magnetic field [1,10,11]. An external magnetic field effect the evolution of the total spin of triplet pairs. Thus, three of nine possible combinations of the triplet pairs in the zero-field have triplet component and only one combination represents the singlet component. In a magnetic field, at the time of formation of the triplet pair, the spins combine in such a manner that the singlet component is distributed over a larger number of states of the pair and to six spin, combinations can include a singlet component. At high external magnetic field only two spin states of the pair have a singlet component. Thus, the triplet annihilation rate should first increase with increasing field, and then fall in strong fields up to a value less than in zero field.

Stage of spatial separation of excitons unreacted at the first meeting is an important step in the process of spin-selective pair annihilation of triplet excitons. After this stage triplet excitons can migrate separately up to possible repeated interaction. The change of total spin state of a coherent pair of excitons occurs in the meantime. This can lead to the formation of the desired spin component for the occurrence of TTA. At this stage the control of spin dynamics under the influence of an external magnetic field is possible for the implementation of the annihilation reaction. Probability of repeated meeting of reagents may depend on the spatial dimension of the system and efficiency of excitons migration.

The aim of this paper is to study the triplet–triplet annihilation in 1,2-benzanthracene molecules adsorbed on nanoporous glasses. One may expect that the pore size and topology of the inner surface would impose certain restrictions on the geometry

$$T_1 + T_1 \underset{k_{dis}}{\overset{k_{coll}}{\leftrightarrows}} {}^{1,3,5}[T_1 \ldots T] \begin{cases} \nearrow {}^{1,5}[T_1 \ldots T_1] \xrightarrow{k_{annih}\left|C_S^1\right|^2} S_1 + S_0 \rightarrow 2S_0 + h\nu_{DF} \\ \searrow {}^{3}[T_1 \ldots T_1] \xrightarrow{k_{annih}\left|C_T^1\right|^2} T_n + S_0 \end{cases} \quad (1)$$

of the adsorbed molecular systems and the migration behaviour of triplet excitons. Direct contact of migrating triplet excitons at TTA and modulation of its rate by a magnetic field can be used as a sensitive tool for probing the structural features of nanoporous materials and specificity of the reactions in nanodisperse systems.

If the molecules in nanopores glass form clusters with a structure close to that of the crystal, the specificity of walks of triplet exciton in such clusters will be close to the dynamics of exciton migration in molecular crystals. It should lead to the magnetic effects that are characteristic of crystals. However, the structural disorder is present in the molecular clusters. In this case a temperature dependence of ADF and magnetic effects corresponding to locally inhomogeneous structures should be expected.

2. Experimental

Borosilicate glass samples with composition $Na_2O–B_2O_3–SiO_2$ (courtesy of Institute of Glass Chemistry, Russian Academy of Sciences) and three different pore sizes, 2.5, 3.9 and 11.1 nm, were used as the porous matrices denoted as Glass I, Glass II and Glass III, respectively, in the form of square slides, 5×5 mm^2 and 0.5 mm in thickness. Structural characterisation of glasses was carried out by measuring low temperature (77.4 K) nitrogen adsorption–desorption isotherms at relative pressure p/p_0 from 10^{-4} to 0.99 with a Sorptomatic-1990 (Thermo Electron Corporation) adsorption analyser. Before measurements, samples were degassed at $\sim 10^{-3}$ Torr and 130 °C for 6–8 h to remove the surface moisture and other possible contaminants.

Specific surface area (S_{BET}) was determined by the Brunauer–Emmett–Teller (BET) method [36]. It was 116, 268 and 190 m^2/g for Glass I, II and III, respectively. Pore size distributions (PSD) were calculated using molecular non-local density functional theory (NLDFT) method with the cylindrical pore model [37] (Quantachrome software, version 2.02) (Fig. 1).

Aromatic hydrocarbon molecule 1,2-BA molecules was used as organic additive. The nature of the electron-excited states and spectroscopic properties of the 1,2-BA molecules were studied by various authors [38–41].

Adsorption of 1,2-benzanthracene molecules onto porous glasses was carried out from a hexane solution at concentration $C = 10^{-4} - 10^{-2}$ mol/l. A glass sample was placed in the solution for 1 h, and then it was dried in an oven for 2 h at 100 °C. The amount of adsorbed 1,2-BA molecules was determined from the optical density of the solution before and after sorption.

Photoexcitation of adsorbed 1,2-BA molecules was carried out by the third harmonic of a Nd laser LCS-DTL-374QT ($\lambda_{ex} = 355$ nm, $\tau = 7$ ns, $E = 5$ μJ). Spectral and kinetic measurements were performed in a photon counting mode. The temperature effects were studied by placing samples in an evacuated optical cryostat.

To determine the effect of the external magnetic field (EMF) the registration of the decay kinetics of delayed fluorescence was carried out with or without the EMF applied. Initially measurements were carried out five-ten times without the field. After that an electromagnet was switched on and the kinetics of the delayed

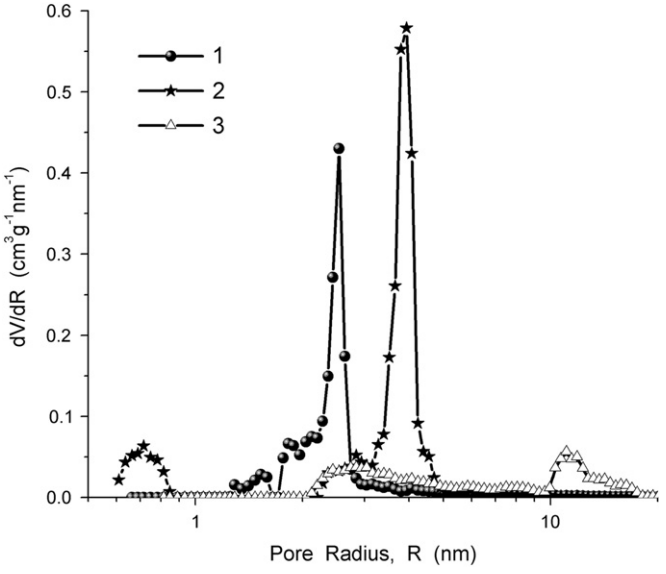

Fig. 1. NLDFT pore size distributions calculated with the model of cylindrical pores using the nitrogen adsorption–desorption isotherms for glasses I (1), II (2) and III (3) at $S_{BET} = 116$, 268 and 190 m^2/g, and average pore radius 2.5, 3.9 and 11.1 nm, respectively.

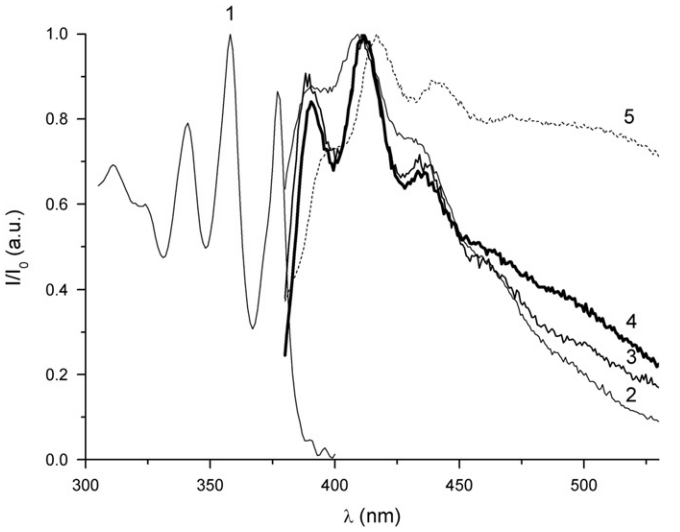

Fig. 2. Absorption spectra (1) and fluorescence spectra of 1,2-BA molecules (2–5) in ethanol (1 and 2) and adsorbed onto porous glasses (3–5): (3) glass I, $C_{BA}=3.2\times10^{-4}$ mol/l; (4) glass I, $C_{BA}=3.8\times10^{-2}$ mol/l, and (5) glass II, $C_{BA}=4.2\times10^{-4}$ mol/l.

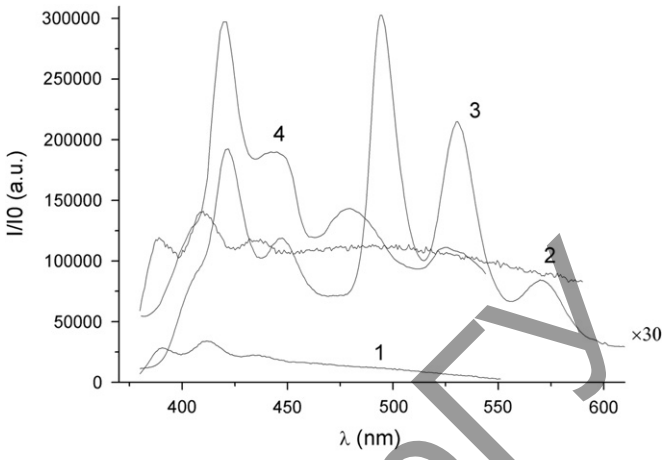

Fig. 3. The concentration dependence of fluorescence spectra of 1,2-BA molecules adsorbed onto glass III: (1) $C_{BA}=5.3\times10^{-3}$ mol/l, (2) $C_{BA}=2.3\times10^{-2}$; and (3) $C_{BA}=0.1$ mol/l. Spectrum of molecular crystal of 1,2-BA (4).

fluorescence annihilation was measured at least five times for each value of the field induction. After each measurement the electromagnet was switched off. The procedure was repeated at different values of the magnetic induction B. The obtained data were averaged for each B value, and the magnetic effect $g(B)$, determined by Eq. (2) was estimated as a relative change in the intensity of the delayed fluorescence in the presence and in the absence of EMF using the following equation:

$$g(B)=\frac{I_B-I_0}{I_0}\times 100\% \qquad (2)$$

where I_B and I_0 are the intensities of delayed fluorescence in the field and without the field, respectively.

3. Results and discussion

All three glasses have PSD peaks around the values given by the supplier, however glass II and glass III have additional peaks at the lower R (pore radius) values (Fig. 1). Glass I has more uniform PSD, whereas glass II, beside the main peak at $R=3.9$ nm has more narrow pores at $R<1$ nm (Fig. 1). Glass III has two broad peaks at $R=10$–11 nm and ca. 3 nm. These structural features can affect the photochemical behaviour of the adsorbed 1,2-BA molecules because of enhanced confined space effects in narrower pores and changes in the intermolecular interactions between adsorbed molecules.

Absorption (curve 1) and the fluorescence of 1,2-BA in ethanol with a concentration 10^{-5} mol/l (curve 2) and in glasses I, II (curves 3–5) are shown in Fig. 2. The resulting absorption and fluorescence spectra have a strong vibronic structure characteristic of aromatic hydrocarbons and coincide with those of other authors for the 1.2-BA molecules [38,39]. The fluorescence spectra of 1,2-BA molecules in the porous glass shift slightly towards longer wavelengths in comparison with the ethanol solution (Fig. 2). Red shift of the fluorescence spectra in porous glass indicates the formation of 1,2-BA molecules in solid clusters. Changing of the intermolecular interactions both within the cluster and with the surrounding matrix leads to a shift of the electronic levels of 1,2-BA molecules [42].

A red-shifted excimer fluorescence band of 1,2-BA molecules appears in the spectrum with increasing of luminophore concentration in the pores. Excimer fluorescence is observed in crystals and concentrated solutions of aromatic hydrocarbons [1,43].

The fluorescence spectra of 1,2-BA molecules adsorbed onto glass III with broader pore sizes from solution at concentration $C_{BA}=5.3\times10^{-3}$ and 2.3×10^{-2} mol/l are similar in the shape and position of bands to the fluorescence spectra of 1,2-BA molecules adsorbed onto glasses I and II with narrower pore sizes (Fig. 3, spectra 1 and 2). A very intensive fluorescence band at $\lambda_{max}=$ 425 nm (curve 3) was observed at $C_{BA}=0.1$ mol/l. It should be noted that the position of the fluorescence band at $\lambda_{max}=425$ nm practically coincides with the band in the spectrum of fluorescence of the molecular crystal of 1,2-BA (Fig. 3, spectrum 4).

Three other intense fluorescence bands with peaks at 495, 530 and 572 nm were registered in the excimer emission of 1,2-BA molecules adsorbed from 0.1 mol/l solution on glass III (Fig. 3, spectrum 3). In this case observed bands belongs to the eximer centres of different spatial configurations [44].

The fluorescence spectral data show that the adsorbed 1,2-BA molecules forms solid-state nanostructures in the glass nanopores. In narrower pores of glasses I and II, 1,2-BA molecules clusters of amorphous structure are formed. 1,2-BA molecules adsorbed in broader pores of glass III forms crystallites and excimer centres along with amorphous clusters, the former becoming particularly noticeable with increasing surface content of the adsorbate. The presence of excimers of different structures in the glass suggests that wide pores have less restriction on the structure of molecular clusters than the narrow pore.

Delayed fluorescence was observed at pulsed laser photoexcitation of 1,2-BA molecules adsorbed onto evacuated glasses. The delayed fluorescence spectra coincide with the spectra of fast fluorescence of the corresponding samples. The observed delayed fluorescence should be attributed to the annihilation delayed fluorescence arising as a result of annihilation of migrating triplet excitons of 1,2-BA molecules.

The ADF intensity decay curves of 1,2-BA molecules adsorbed in glass pores are shown in Fig. 4. The initial part of the kinetics of fluorescence decay can be described by a power function, and the long-term part is described by the exponential function for 1,2-BA molecules adsorbed on all glasses studied independently of the pore size or the concentration of the adsorbed 1,2-BA molecules. The exponent values of the power function (n) and duration of fluorescence (τ) calculated using the exponential part of the kinetic curves of ADF, are presented in Table 1. As shown in Ref. [1] for the formal-kinetic model at high power optical

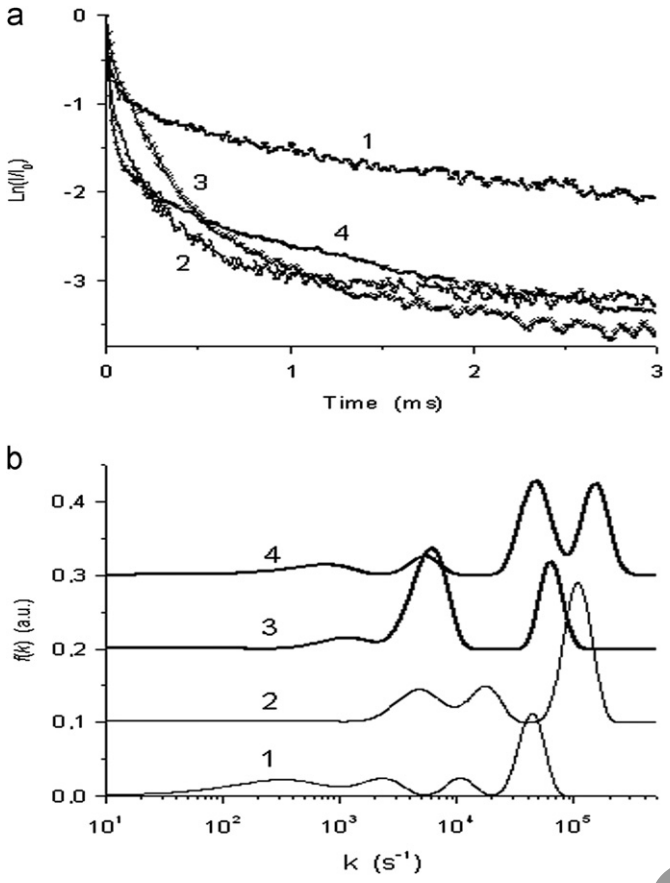

Fig. 4. (a) The decay kinetics of ADF 1,2-BA molecules adsorbed at $T=100$ K on glasses: (1) I, $C_{BA}=3.8\times10^{-2}$ mol/l, (2) II, $C_{BA}=3.2\times10^{-2}$ mol/l, (3 and 4) III, $C_{BA}=(3)\ 2.3\times10^{-2}$ and (4) 0.1 mol/l; (b) the distribution function of the reaction rate constant.

Table 1
Values that characterise the kinetics of delayed fluorescence of the 1,2-BA molecules in porous glass.

Glass	C (mol/l)	T (K)	n	τ (ms)	h_1 (0.01–0.1) (ms)	h_2 (1.0–5.0) (ms)
I	3.8×10^{-2}	100	0.4	3.7	0.4	0.6
		200	0.6	3.6	0.4	0.6
II	3.2×10^{-2}	100	0.6	4.0	0.5	0.6
		200	0.6	3.0	0.6	0.6
III	9.1×10^{-4}	100	0.2	7.0	0.25	1.0
		200	0.5	3.8	0.35	1.0
	2.3×10^{-2}	100	0.5	2.2	0.25	1.0
		200	0.5	2.0	0.5	1.0
	10^{-1}	100	0.75	2.4	–	–
		200	1.2	0.5	–	–

excitation, when the decrease of triplet electronic excitation occurs mainly due to bimolecular decay kinetics of the attenuation obeys a power law. The index n is equal to 2, when the rate of decay of bimolecular channel of electronic excitations triplet is much higher than the rate of monomolecular decay. Value of the index n calculated from the decay kinetics ADF decreases for increasing the share of monomolecular decay channel.

At 100 K the n value varies only slightly between glass samples with different PSD but similar contents of the adsorbed 1,2-BA molecules. This value increases in the initial part of the decay curve for 1,2-BA molecules adsorbed onto glass III at $C_{BA}=0.1$ mol/l. The long-term parts of the decay curves for 1,2-BA molecules adsorbed onto glasses I and II have practically identical τ. The τ value decreases for 1,2-BA molecules adsorbed on glass III.

It was shown [45,46] that the local structural heterogeneity of multilayer Langmuir–Blodgett films of aromatic molecules leads to the dispersion of the triplet levels that is manifested in the temperature dependence of the rate of migration of triplet excitons.

The distribution functions of the reaction rate constant $f(k)$ for the decay kinetics of ADF (Fig. 4b) were calculated using the following integral equation:

$$I_{DF}(t)=\int_{k_{min}}^{k_{max}} f(k)\exp(-kt)\mathrm{d}k, \tag{3}$$

where k_{min} and k_{max} are the minimal and maximal k values in integration. Solution of Eq. (3) is well known ill-posed problem due to the impact of noise on measured data, which does not allow one to utilise exact inversion formulas or iterative algorithms. Therefore, Eq. (3) was solved using a regularisation procedure based on the CONTIN algorithm [47] under nonnegativity condition ($f(k)\geq 0$ at any k) and an unfixed value of the regularisation parameter (α) determined on the basis of the F-test and confidence regions using the parsimony principle.

The heterogeneity of both the pore size distribution (Fig. 1) and 1,2-BA molecular cluster structure in these pores causes the complex shape of the $f(k)$ function with three to four peaks (Fig. 4).

A monotonic decrease in the emission intensity with a small shoulder in the range from 200 to 220 K is observed with increasing temperature (Fig. 5, curve 1) for 1,2-BA molecules adsorbed on glass I. The temperature dependence of the ADF (curves 2 and 3) has a significant maximum for 1,2-BA molecules adsorbed on glass

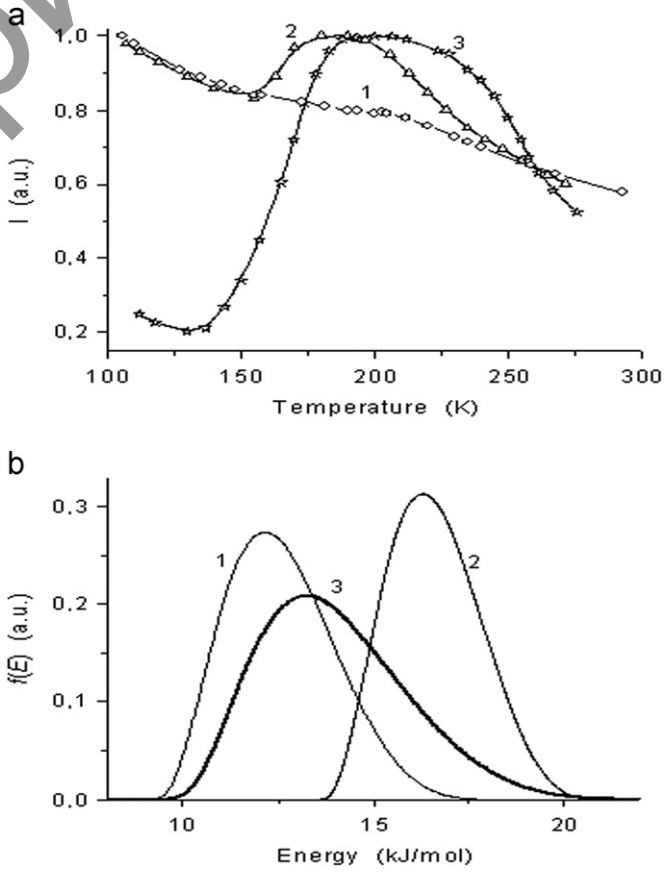

Fig. 5. (a) Temperature dependence ADF intensity of 1,2-BA molecules in porous glasses: (1) I, $C_{BA}=3.8\times10^{-2}$ mol/l, (2, 3) III at (2) $C_{BA}=9.1\times10^{-4}$ and (3) 10^{-1} mol/l; and (b) the distribution function of the triplet level dispersion energy.

III. The triplet level dispersion increases with increasing amount of 1,2-BA molecules adsorbed in the pores. For the temperature range, in which the intensity of the ADF increases, non-homogeneous broadening of triplet levels can be described by the following equation:

$$I_{DF} = I_0 \exp\left(\frac{-\Delta E}{kT}\right) \tag{4}$$

where I_0 is the intensity of delayed fluorescence at 100 K, I_{DF} is the current ADF value and ΔE is triplet level dispersion value. To consider the nonuniformity of the systems, Eq. (4) can be transformed into integral equation:

$$I_{DF}(t) = \int_{E_{min}}^{E_{max}} f(E)\exp\left(\frac{-E}{R_g T}\right) dE, \tag{5}$$

where E_{min} and E_{max} are the minimal and maximal E values in integration, R_g is the gas constant. Eq. (5) was solved using the CONTIN algorithm similar to solution of Eq. (3).

From the results obtained it follows that the dispersion of the triplet energy levels depends on the concentration of molecules in the pores. The structure of the adsorbate cluster becomes more heterogeneous with increasing concentration, which is reflected by broadening of the $f(E)$ distribution (Fig. 5b). In narrower pores of glass I molecules of 1,2-BA form quasi-one-dimensional chain structure. As evidenced by the absence of a pronounced maximum on the temperature dependence of ADF intensity, the local environment of the luminescent centres remains uniform. A monotonic decrease in the yield of fluorescence with increasing temperature is related to intensification of intra- and intermolecular processes leading to nonradiative deactivation of the triplet centres. The local environment around each molecule changes both in larger pores of glass III and with increasing adsorbate concentration inside pores, causing nonuniform broadening of triplet levels. Increasing temperature leads to the emission of excitons from their traps, and facilitates their migration and the formation of triplet pairs.

For curve fitting of the kinetics of ADF decay in the clusters of 1,2-BA molecules in nanopores, we applied a combination of the formal kinetics and percolation [14,48] models. This approach was used previously to describe the annihilation of triplet excitons of aromatic molecules in Langmuir–Blodgett films, which followed nonexponential decay kinetics of ADF [33,34]. Our analysis showed that the initial part of the experimental kinetic curves is well approximated by a power function with power index $n=0.2$–0.6 at lower concentrations of adsorbed 1,2-BA molecules irrespective of pore size in the selected range of temperatures. For homogeneous media, the fact that the initial part of the kinetics of decay can be described within the formal kinetics model points to the annihilation of migrating excitons in nanoclusters with a structure close to crystalline. Evidently, the number and size of the "crystalline" clusters increases at high concentrations (~0.1 mol/l) of the adsorbed 1,2-BA molecules in larger pores. This leads to an increase in the rate constant of the triplet excitons annihilation which is manifested in increasing power index n up to 0.75 and 1.2 at temperatures of 100 and 200 K, respectively (Table 1).

TTA rate constant related to the percolation clusters becomes a time-dependent parameter [14,48,49], and the reaction of TTA is given by:

$$\frac{d[T]}{dt} = -k(t)\,[T]^2 \tag{6}$$

The TTA reaction rate coefficient $k(t)$ is expressed by the dependence:

$$k(t) \sim \frac{dS(t)}{dt} \sim t^{-h}, \quad 0 \le h \le 1, \tag{7}$$

where $S(t)$ is the number of locations visited by the excitation in the process of random walks. Parameter h characterises the degree of local inhomogeneity. Its lower limit, $h=0$, corresponds to the motion in a homogeneous medium, and the upper limit $h=1$ characterises the motion in locally heterogeneous clusters.

Given the fact that the phosphorescence intensity I_{Ph} is proportional to the density of triplet excitations, and the intensity of ADF I_{DF} is proportional to the concentration of triplets, the time dependence of $k(t)$ can be found from the following relationship:

$$\frac{I_{DF}}{I_{Ph}^2} \sim k(t) \sim t^{-h} \tag{8}$$

The plot $\ln(I_{DF}/I_{Ph}^2)$ vs. $\ln(t)$ must be linear with slope h. The dependence of $I_{DF}(t)$ on $I_{Ph}(t)$ can be obtained experimentally. In the absence of phosphorescence, the parameter h can be determined from the plot of $\ln(I_{DF})$ vs. $\ln(t)$. This gives a less accurate value of h, but qualitatively the trend remains unchanged.

The description of the decay kinetics of ADF using a percolation model is shown in Fig. 6. In the temperature range of 100–200 K, the entire time interval can be divided into two regions, with linear dependence of $\ln(I_{DF})$ on $\ln(t)$ but with a different slope (h) (Fig. 6). The initial part of the kinetic curve (up to 0.1 ms) is characterised by a linear plot with a small slope. At 100 K $h_1=0.25$, which corresponds to the exciton migration in a medium with a homogeneous structure. Increasing temperature of glass leads to the migration of excitons typical of a percolation cluster near the percolation threshold ($h=0.33$) [50].

An increase in the value of h_1 with increasing concentration of the molecules adsorbed in pores (Table 1) indicates enhancement of the local heterogeneity in the crystalline clusters, in which the annihilation of excitons occurs.

In the millisecond range, the h_2 values changed from 0.6 to 1 with increasing concentration of the adsorbate. It reveals the annihilation of triplets in the percolation clusters with a significant local heterogeneity. It should be noted that at temperatures above 200 K for all glasses the two regions merge into one and the complete kinetics of ADF is described by a linear dependence of $\ln(I_{DF})$ vs. $\ln(t)$ with a slope of $h \approx 0.5$ for all concentrations studied. The value $h \approx 0.5$ coincides with the value obtained for solid solutions of chrysene, a polyaromatic hydrocarbon [50].

Therefore, it can be concluded that at temperatures above 200 K the adsorbed 1,2-BA molecules are arranged in structures, which have similar size and topology regardless of the pore size.

Thus, the data obtained prove that the adsorption of aromatic molecules in nanopores of glass leads to formation of molecular

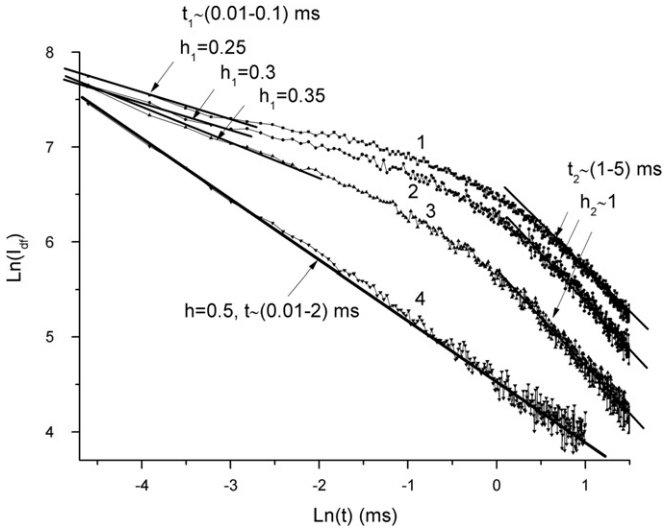

Fig. 6. Description of the decay kinetics with ADF (glass III) percolation model [48] at temperatures: (1) 100, (2) 140, (3) 180, and (4) 235 K.

clusters in the adsorption layer. Annihilation triplets in the clusters with a homogeneous structure dominate in the initial stage of the ADF. In the millisecond range, the ADF kinetics is formed by triplet excitons straying in the percolation clusters. The conclusion about the fractal nature of the distribution of dye molecules in nanoporous glass is based on the study of the intermolecular energy transfer [51].

Further details regarding random walks and molecular interactions in nanosized pores can be obtained by studying the modulation of the TTA rate constant with an external magnetic field [52,53]. An important step in the spin-selective pair annihilation of triplets is the spatial divergence of a non-annihilated pair at their first encounter. During this time, a change in the total spin state of a coherent pair of triplets occurs, which can be influenced by the external magnetic field. Their second encounter can lead to a successful interaction provided a sufficient spin component is available. The probability of this secondary event depends on the system dimension, the migration efficiency of excitons and their interaction. Effects of the magnetic field on the annihilation of migrating excitons and diffusion of triplet molecules in crystals and liquids were studied in detail and discussed elsewhere [10–13,53].

The influence of EMF on the kinetics of ADF of 1,2-BA molecules adsorbed in porous glasses was studied at different temperatures. The magnetic field was directed tangentially to the substrate surface along its short side. Evaluation of the magnetic field effects was performed by measuring the "instantaneous" intensity at different times after excitation.

The negative magnetic effect observed for glasses I and II at all concentrations and for glass III at C_{BA} below 0.1 mol/l, is characteristic of disordered systems (Fig. 7, curves 1–3). The positive magnetic effect is observed for glass III with largest nanopores at $C_{BA}=0.1$ mol/l (Fig. 7, curve 4), which is characteristic of crystal structures [10]. It should be noted that the magnetic effect for all samples is independent of the time of registration at 100 K. The results show that the magnetic effect $g(B)$ (Eq. (1)) increases with increasing pore size (curves 1–3).

The experimental results show that the pore size of the glass matrix and concentration of 1,2-BA molecules significantly affect the nature and magnitude of the observed magnetic effects. Positive magnetic effect is present in some samples. Positive $g(B)$ shows the presence of clusters in the pores of the ordered molecular orientation. We have made evaluation of the degree of ordering of molecular clusters, using the analytical expressions given in Ref. [35]. The analysis of data on the effect of magnetic field on the ADF at $T=100$ K. The analysis showed that only the glass III at concentration $C_{BA}=0.1$ mol/l (Fig. 6, curve 4) the degree of ordering of clusters is 50%. The degree of disorder in the cluster cannot be calculated for the remaining samples. Positive magnetic effect is not for them (curves 1–3). As part of the model the growth of $g(B)$ with the increase of the pore diameter can be related to the difference in the degree of disorder in the orientation of the molecules or the change in the ratio of the dissociation rate constants and triplet–triplet annihilation rate (k_{dis}/k_{annih}).

These data are consistent with theoretical analysis [54], which showed that the value of the magnetic modulation of the TTA rate constant increases with increasing pore radius.

The most effective migration of triplet excitons is observed at 200 K. Under these conditions the mean free path of excitons expands during the lifetime of the triplet state, and a large number of centres with different spatial orientation is involved in the annihilation process. These parameters can influence the magnetic effect.

Analysis of the experimental data in the model of [35] gives physically unrealistic results. This may be due to the fact that the triplet annihilation reaction channel is not included in the derivation of analytical expressions in order to simplify them. In the character of the annihilation reaction may contribute to the processes associated with the redistribution of the ratio between the triplet–singlet or triplet–quintet pair states for the time of the trapped exciton [55].

Similar effect of the magnetic field on g(B) is observed at 200 K, if measured at 0.01 ms after the laser pulse (Fig. 8). However, in this case the magnetic effect is substantially decreased (compare curves 3 and 4 in Fig. 7 and curves 4 and 5 in Fig. 8, respectively).

With increasing recording time (1–3 ms) only the negative magnetic effect is observed for all systems studied with an increase in the magnitude of the magnetic effect by 35–40% (Fig. 8, curve 5 vs. curve 6).

We can assume that the observed temperature dependence of $g(B)$ is due to changes in the migration behaviour of triplet excitons in the microcrystalline and percolation clusters.

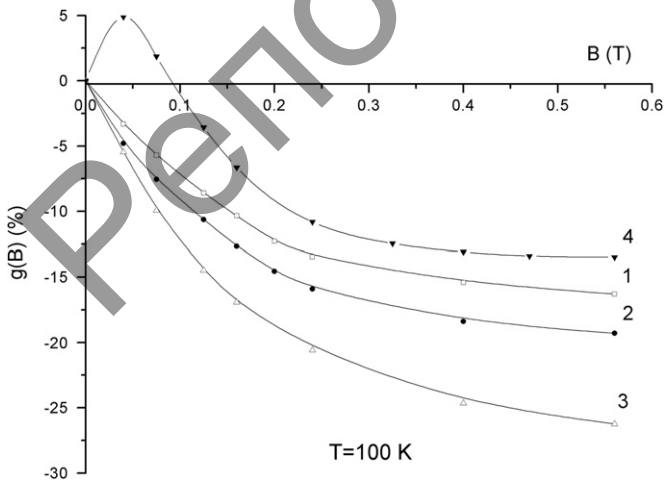

Fig. 7. The effect of the magnetic field on the intensity of the delayed fluorescence at $T=100$ K. $g(B)$ was measured at 0.01 ms after the laser pulse. (1) glass I, $C_{BA}=3.8\times10^{-2}$ mol/l; (2) glass II, $C_{BA}=3.2\times10^{-2}$ mol/l; (3) and (4) glass III, $C_{BA}=2.3\times10^{-2}$ and 0.10 mol/l, respectively.

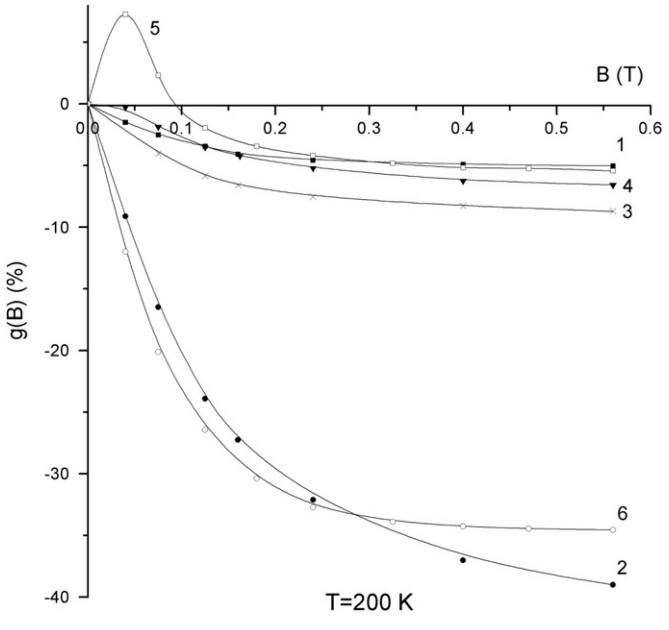

Fig. 8. The effect of the magnetic field on the intensity of the delayed fluorescence at $T=200$ K. $g(B)$ was measured at 0.01 ms after the laser pulse in (1, 3, 4 and 5) and at 1 ms in (2 and 6) 0.1 and (2) glass I, $C_{BA}=3.8\times10^{-2}$ mol/l; (3) glass II, $C_{BA}=3.8\times10^{-2}$ mol/l; (4), (5) and (6) glass III, 2.3×10^{-2} mol/l (4) and 0.10 mol/l (5 and 6).

4. Conclusions

Thus two types of clusters of aromatic molecules are formed in porous glasses. Clusters with the crystal structure dominate in the ADF decay kinetics in the initial period of time (a fraction of a millisecond) after excitation. Amorphous clusters determine the form of fluorescence decay in the millisecond range. The increase in the pore size and concentration of the adsorbate lead to the dominance of crystalline components. The results presented here can be used to develop techniques for probing the structure of the adsorbed layer in nanoporous systems examining the effect of an external magnetic field on the ADF kinetics.

Broadening of the triplet energy levels is observed due to the inhomogeneous structure of molecular clusters. This leads to thermal activation process of TTA. The inhomogeneous broadening of the triplet energy levels increases with the diameter of the pores and the concentration of adsorbed molecules.

The data obtained on the influence of the external magnetic field on the triplet–triplet annihilation rate constant support the results of the kinetic studies. 1,2-benzanthracene molecules adsorbed in nanopores of porous glass form clusters with different structure, which depends on the pore size and the concentration of the adsorbate. During initial time after laser excitation, the largest contribution in triplet–triplet annihilation delayed fluorescence intensity is due to triplet pairs which annihilate in the clusters with ordered arrangement of molecules. This conclusion is mainly based on the dependence of the speed of modulation of the TTA by the external magnetic field that is typical of crystals of aromatic substances [10]. The shape of the decay kinetics in the millisecond range is determined by the pair annihilation of triplets migrating in the percolation clusters. The dependence of the magnetic field effects on the magnetic induction B is similar to the magnetic field modulation of the TTA rate constant in disordered systems [35]. The dependence of these effects on the pore size indicates an important role of the dynamics of convergence and divergence in the annihilation of triplets in confined space of nanopores.

Noteworthy the large value of the negative magnetic effect under effective migration of triplet excitons in randomly oriented molecular clusters. Specific theoretical analysis is necessary for a more complete explanation of the effect of external magnetic field on the reaction of TTA in nanoscale systems with restricted geometry.

Acknowledgements

D. Afanasyev and N. Ibrayev gratefully acknowledge the Ministry of Education and Science of Republic of Kazakhstan Grant no. 196/GF for their financial support.

References

[1] M. Pope, C.E. Swenberg, Electronic Processes in Organic Crystals, Clarendon Press, Oxford, 1982.
[2] V.M. Agranovich, R. Hochstrasser (Eds.), Spectroscopy and Excitation Dynamics of Condensed Molecular System, North Holland, Amsterdam, Netherlands, 1983.
[3] R.F. Khairutdinov, Russ. Chem. Rev. 67 (1998) 109.
[4] M.N. Berberan-Santos, E.N. Bodunov, J.M.G. Martinho, Opt. Spectrosc. 99 (2005) 955.
[5] M.S. Mikhelashvili, A.M. Mikhaeli, J. Chem. Phys. 96 (1992) 4766.
[6] M.S. Mikhelashvili, A.M. Mikhaeli, J. Chem. Phys. 98 (1994) 8114.
[7] M.G. Kucherenko, Coll. J. 60 (1998) 380 in Russian.
[8] B. Minaev, E. Jansson, M. Lindgren, J. Chem. Phys. 125 (11) (2006) 094306.
[9] M. Lindgrena, B. Minaev, E. Glimsdal, R. Vestberg, R. Westlund, E. Malmström, J. Lumin. 124 (2007) 302.
[10] R.E. Merrifield, J. Chem. Phys. 48 (1968) 4318.
[11] R.C. Jonson, R.E. Merrifield, P. Avakian, R.B. Flippen, Phys. Rev. Lett. 19 (1967) 285.
[12] L.R. Faulkner, A.I. Bard, J. Am. Chem. Soc. 91 (1969) 6495.
[13] P.W. Atkins, G.T. Evans, Mol. Phys. 29 (1975) 921.
[14] E.I. Newhouse, R. Kopelman, Chem. Phys. Lett. 143 (1988) 106.
[15] H.L. Tavernier, A.V. Barzykin, M. Tachiya, M.D. Fayer, J. Phys. Chem. B 102 (1998) 6078.
[16] D. Hertela, H. Bassler, R. Guentner, U. Scherf, J. Chem. Phys. 115 (2001) 10007.
[17] A. Gerhard, H. Bassler, J. Chem. Phys. 117 (2002) 7350.
[18] P. Avakian, Pure Appl. Chem. 37 (1974) 1.
[19] A. Suna, Phys. Rev. B 1 (1970) 1716.
[20] V.V. Bryukhanov, G.A. Ketsle, L.V. Levshin, B.F. Minaev, Opt. Spectrosc. 45 (1978) 1090.
[21] G.A. Ketsle, L.V. Levshin, G.V. Melnikov, J. Appl. Spectrosc. 34 (1981) 435.
[22] B.F. Minaev, Sov. J. Phys. 21 (1978) 1120.
[23] A. Serebrennikov, B.M. Abdrahmanov, B.F. Minaev, Russ. J. Phys. Chem. B 5 (1986) 878.
[24] A. Serebrennikov, B.F. Minaev, Sov. J. Phys. 21 (1978) 571.
[25] A. Serebrennikov, B.F. Minaev, Chem. Phys. 114 (1987) 359.
[26] G.A. Ketsle, L.V. Levshin, G.V. Melnikov, B.F. Minaev, Opt. Spectrosc. 51 (1981) 665.
[27] A. Benfredj, S. Romdhane, H. Bouchriha, Synth. Met. 150 (2005) 241.
[28] A. Benfredj, F. Henia, L. Hachani, S. Romdhane, H. Bouchriha, Phys. Rev. B 71 (1) (2005) 075205.
[29] L. Hachani, A. Benfredj, S. Romdhane, M. Mejatty, J.L. Monge, H. Bouchriha, Phys. Rev. B 77 (1) (2008) 035212.
[30] T. Barhoumi, J.L. Monge, M. Mejatty, H. Bouchriha, Eur. Phys. J. B 59 (2007) 167.
[31] E.N. Bodunov, M.N. Berberan-Santos, J.M.G. Martinho, Chem. Phys. 316 (2005) 217.
[32] E.N. Bodunov, M.N. Berberan-Santos, J.M.G. Martinho, Opt. Spectrosc. 100 (2006) 539.
[33] N.Kh. Ibrayev, V.A. Latonin, J. Lumin. 87–89 (2000) 760.
[34] N.Kh. Ibrayev, V.A. Latonin, Phys. Solid State 41 (1999) 664.
[35] J. Mezyk, R. Tubino, A. Mech, F. Meinardi, Phys. Rev. Lett. 102 (1) (2009) 087404.
[36] S.J. Gregg, K.S.W. Sing, Adsorption, Surface Area and Porosity, 2nd ed., Academic Press, London, 1982.
[37] A.V. Neimark, P.I. Ravikovitch, Microporous Mesoporous Mater. 44 (2001) 697.
[38] J.B. Birks, Photophysics of Aromatic Molecules, Wiley Interscience, New York, 1970.
[39] R.N. Nurmukhametov, Russ. Chem. Rev. 35 (1966) 469.
[40] N.A. Borisevich, G.G. Dyachenko, V.A. Petukhov, D.I. Polishchuk, M.A. Semenov, Opt. Spectrosc. 110 (2011) 686.
[41] S.P. McGlinn, T. Adzumi, M. Kinoshita, Molecular Spectroscopy of the Triplet State Englewood Cliffs, Prentice-Hall Inc., New Jersey, 1969.
[42] N.G. Bakhshiev, Spectroscopy of Intermolecular Interactions, Nauka, Leningrad, 1972 in Russian.
[43] J.B. Birks, L.G. Christophorou, Proc. R. Soc. 274 (1963) 552.
[44] J. Hoffman, K.P. Scefeld, W. Horberger, H. Bassler, Mol. Phys. 37 (1979) 973.
[45] N.Kh. Ibrayev, Opt. Spectrosc. 93 (2002) 242.
[46] N.Kh. Ibrayev, K.M. Makhanov, Mol. Cryst. Liq. Cryst. 384 (2002) 25.
[47] S.W. Provencher, Comput. Phys. Commun. 27 (1982) 213.
[48] L.A. Harmon, R. Kopelman, J. Phys. Chem. 94 (1990) 3454.
[49] I.M. Sokolov, Sov. Phys. Usp. 29 (1986) 924.
[50] S.A. Bagnich, Chem. Phys. 237 (1998) 359.
[51] T.V. Antropova, A. Gordeeva, B.D. Ryzhikov, A.M. Saletsky, J. Appl. Spectrosc. 72 (2005) 446 in Russian.
[52] K.M. Salikhov, A.L. Buchachenko, N. Molin, R.Z. Sagdeev, Magnetic and Spin Effects in Chemical Reaction, Elsevier, Amsterdam, Netherlands, 1983.
[53] B. Zel'dovich, A.L. Buchachenko, E.L. Frankevich, Sov. Phys. Usp. 31 (1988) 385.
[54] M.G. Kucherenko, R.N. Dusembaev, Chem. Phys. Mesoscopic 12 (2010) 1 in Russian.
[55] J. Funfschilling, L. Altwegg, I. Zschokke-Granacher, M. Chabr, D.F. Williams, J. Chem. Phys. 70 (1979) 4622.